Characterization of dual agonists for kinin B1 and B2 receptors and their biased activation of B2 receptors

Xianming Zhang[a], **Jessica L. Lowry**[a], **Viktor Brovkovych**[a], and **Randal A. Skidgel**[a,b,*]

[a]Department of Pharmacology, University of Illinois at Chicago College of Medicine, Chicago, Illinois 60612

[b]Center for Lung and Vascular Biology, University of Illinois at Chicago College of Medicine, Chicago, Illinois 60612

Abstract

Kinin B1 and B2 receptors (kB1R and kB2R) play important roles in many physiological and pathological processes. In some cases, kB1R or kB2R activation can have overlapping or complementary beneficial effects, thus an activator of both receptors might be advantageous. We found that replacement of the C-terminal Arg in the natural kB2R activators bradykinin (BK) or kallidin (KD) with Lys (K^9-BK or K^{10}-KD) resulted in agonists that effectively stimulate the downstream signaling of both the kB1R and kB2R as measured by increased inositol turnover, intracellular calcium, ERK1/2 phosphorylation, arachidonic acid release and NO production. However, K^9-BK and K^{10}-KD displayed some characteristics of biased agonism for kB2Rs as indicated by the rapid kinetics of ERK1/2 phosphorylation induced by K^9-BK or K^{10}-KD compared with the prolonged response mediated by BK or KD. In contrast, kinetics of ERK phosphorylation stimulated by K^{10}-KD activation of the kB1R was as same as that induced by known kB1R agonist des-Arg^{10}-KD. Furthermore, the endocytosis of kB2Rs mediated by K^9-BK and K^{10}-KD was remarkably less than that induced by BK and KD respectively. K^{10}-KD stimulated kB1R and kB2R-dependent calcium responses and ERK1/2 phosphorylation in bovine endothelial cells. In cytokine-treated human endothelial cells, K^{10}-KD stimulated ERK1/2 phosphorylation and a transient peak of NO production that was primarily kB2R-dependent. K^{10}-KD also stimulated prolonged NO production that was both kB1R and kB2R-dependent. These data provide the first examples of dual agonists of kB1R and kB2R, and a biased agonist of kB2R and may provide useful clues for developing dual modulators of kB1Rs and kB2Rs for potential therapeutic use.

Keywords

Kinin B1 receptor; kinin B2 receptor; biased agonist; kinin peptides; G protein–coupled receptors; endocytosis

*Corresponding author and address: Randal A. Skidgel, Ph. D., Department of Pharmacology (m/c 868), University of Illinois College of Medicine at Chicago, 835 S. Wolcott, Chicago, IL 60612, Tel: 312-996-9179, Fax: 312-996-1648, rskidgel@uic.edu.

1. Introduction

Bradykinin (BK) or kallidin (KD) are 9 or 10 amino acid peptides released kininogen precursors by plasma or tissue kallikrein that selectively activate the kinin B2 receptor (kB2R) [1, 2]. The C-terminal Arg of BK or KD can be cleaved by membrane carboxypeptidase M (CPM) or plasma carboxypeptidase N (CPN) to generate des-Arg[9]-BK (DABK) or des-Arg[10]-KD (DAKD), which are not kB2R agonists, but instead specifically activate the kinin B1 receptor (kB1R) [2–7]. Thus, the presence or absence of the basic C-terminal Arg of BK and KD is a key determinant of their selectivity for the two kinin receptors. The kB1R and kB2R have 36% sequence identity in humans and belong to the family of seven transmembrane receptors, coupling to G protein subtypes $G\alpha q$ and $G\alpha i$ [2, 7].

kB1R and kB2R play key roles in many pathological or physiological processes including nociception, inflammation, and cardiovascular and renal diseases [2, 8–11]. For example, kB2R knockout mice have hypertension and exaggerated blood pressure increases induced by angiotensin II and chronic salt loading [12]. kB2R knockout mice develop age-related heart failure due to left ventricular remodeling [13]. kB1R signaling reduces blood pressure in kB2R knockout mice although kB1R knockout alone does not alter normal blood pressure [14]. Diabetic nephropathy was also markedly enhanced in kB2R knockout mice [15] and renal injury due to ischemia/reperfusion was markedly worse in kB1R and kB2R double knockout mice compared with kB2R knockout or wild type mice [16]. These data indicate beneficial roles for kB1R and kB2R signaling in the cardiovascular and renal systems. In contrast, kB1R and kB2R activation can have deleterious effects, causing pain and inflammation. For example, both kB1R and kB2R are involved in nociception as kB2R agonist BK induced thermal hyperalgesia in kB1R knockout mice and kB1R agonist DABK induced the thermal hyperalgesia in kB2R knockout mice [17]. kB1R also regulates pain by facilitating the nociceptive spinal reflex, as it was decreased in kB1R knockout mice [18]. The kB1R and kB2R also regulate the recruitment and infiltration of inflammatory cells into local tissues. For example, in experimental autoimmune encephalomyelitis, leukocytes infiltrating into the central nervous system were decreased in kB2R knockout mice whereas T helper type 17 cells were reduced in kB1R knockout mice [19, 20].

Because of the potential roles of these receptors in various diseases, numerous agonists and antagonists of kB1R or kB2R have been developed [21–24], with most of them being derivatives of the natural kinin peptides [2], but some low molecular weight non-peptide ligands have also been produced [2, 24]. These ligands generally have high selectivity for either the kB1R or kB2R [2]. However, in cases where kB1R and kB2R activation results in overlapping or complementary responses [12, 14, 17, 19, 20], ligands that bind to both kB1R and kB2R might be more therapeutically efficacious. B9430 (D-Arg-[Hyp[3], Igl[5], D-Igl[7], Oic[8]]-BK) was developed as a dual antagonist of both the kB1R and kB2R [25], but dual agonists of kB1R and kB2R have not been described. Although KD can bind with a relatively high affinity to both human receptors [2], it is either much less potent or inactive in stimulating kB1R-dependent responses [3, 26–29]. A complicating factor in studies assessing the activity of KD on kB1Rs is the possible conversion of added KD to the potent kB1R agonist DAKD by cellular carboxypeptidases such as the widely expressed carboxypeptidase M [4, 30, 31]. In fact, we found that in transfected HEK cells stably expressing only kB1Rs, KD was inactive in stimulating a calcium response, but became a potent kB1R agonist in cells co-expressing CPM and kB1Rs [3, 27].

G protein-coupled receptor activation by agonists was initially thought to convert the receptor from an "off" state to a fully "on" state that would then activate all associated downstream pathways. However, more recently it has been discovered that some agonists

may activate only a subset of possible receptor responses, which has been termed "biased agonism" or "ligand bias" [32, 33]. Furthermore, agonists may exhibit bias in their ability to stimulate receptor desensitization and endocytosis [32, 33]. Biased agonists have been well characterized for several G protein-coupled receptors, but have not been identified for the kinin receptors.

Because the presence or absence of the C-terminal Arg of BK and KD is a key switch for selectivity with the kB1R or kB2R, we tested the agonist activity of BK and KD in which the C-terminal Arg was replaced with lysine (K^9-BK and K^{10}-KD). Surprisingly, we found that K^9-BK and K^{10}-KD effectively stimulate both kB1R and kB2R signaling, but had biased effects on kB2R-mediated ERK activation. These findings provide promising clues for development of dual kB1R and kB2R agonists that could be useful therapeutic agents for treatment of cardiovascular diseases.

2. Materials and Methods

2.1. Materials

Low-glucose Dulbecco's Modified Eagle's Medium (DMEM) and HAM's F-12 medium were obtained from GIBCO/Life Technologies. Fetal bovine serum (FBS) was from Atlanta Biologicals. HOE-140, des-Arg^9-HOE-140, BK, des-Arg^9-BK, des-Arg^{10}-KD and des-Arg^{10}-Leu^9-KD were from Sigma. KD was from Bachem. K^9-BK and K^{10}-KD were synthesized by Chi Scientific. [^{3}H]-Des-Arg^{10}-KD was from PerkinElmer. [^{3}H]-BK was from Amersham Biosciences. The primary sequence of peptides used is summarized in Table 1. [^{3}H]-Arachidonic acid and myo-[^{3}H]inositol were from American Radiolabeled Chemicals, Inc. Fura-2/AM was from Molecular Probes. Anti-ERK1/2 and anti-phosphorylated ERK1/2 antibodies were from Cell Signaling. Goat anti-mouse and anti-rabbit IgG conjugated-HRP were from Pierce. Common chemicals were from Fisher Scientific.

2.2. Cells

Human embryonic kidney (HEK293) and Chinese hamster ovary (CHO) cells were from the American Type Culture Collection. Cells were maintained in DMEM or F-12 containing 100 U/ml penicillin, 100 μg/ml streptomycin and 10% FBS. Bovine pulmonary artery endothelial cells (BPAEC) were from Genlantis and were maintained in DMEM containing 100 U/ml penicillin, 100 mg/ml streptomycin and 15% FBS. Primary human lung microvascular endothelial cells (HLMVEC) were from Lonza and cultured in flasks coated with 0.1% gelatin in Endothelial Cell Basal Medium (EBM®-2, Lonza) supplemented with EGM®-2 SingleQuots® kit (Lonza) and 10% fetal bovine serum (Atlanta Biologicals). Cells were maintained at 37°C in a humidified atmosphere of 5% CO_2 and HLMVEC between passage 3 and 6 were used for assay.

2.3. Generation of receptor constructs

The cDNA for human kB1R was a gift from Dr. Fredrik Leeb-Lundberg (University of Lund, Sweden) and for human kB2R was from Syntex Co. The cDNA of human CPM was cloned by our lab [34]. Wild type kB1R, kB2R or CPM were cloned into pcDNA3 or pcDNA6 vectors (Invitrogen) for expression in mammalian cells. kB1R was also cloned into pIRES (Clontech) at the Nhe I/Xho I sites, together with EGFP at the Sal I/Not I sites, to achieve the coexpression of kB1R and GFP separately, but at the same time in the same cells [3]. kB2R-YFP was generated as described by Chen et al. [35]. All the PCR fragments used were amplified using high fidelity Taq DNA polymerase. Constructs were verified by DNA sequencing performed by the DNA Services Facility of the Research Resources Center, University of Illinois at Chicago.

2.4. Transfection and establishment of stable cell lines

HEK293 cells, at 70–80% confluence in 6-well plates, were transfected with SuperFect (Invitrogen) reagent containing 5 μg DNA according to the manufacturer's instructions. After 48 h, cells were transferred to selective medium containing G418 (500 μg/ml) or blasticidin (5 μg/ml) according to the resistance gene contained in the vector. The cells were cultured for 15–30 days in selective medium, and then diluted for single clone selection. For kB1R and kB2R selection, the increase in $[Ca^{2+}]_i$ stimulated by their specific agonist (DAKD or DABK, respectively) was evaluated for each clone [3]. The cDNA of kB2R-YFP was transfected into CHO cells, and the appropriate clones were selected in HAM's F-12 medium supplemented with blasticidin (5μg/ml). Cells that highly expressed YFP were separated by fluorescence-activated cell sorting with an Elite ESP cell sorter (Coulter Corp.). The function of kB2R-YFP was confirmed by measuring arachidonic acid generation after stimulation with BK [35]. For CPM selection, the enzyme activity was determined as described [3] and expression was confirmed by Western blotting.

2.5. Measurement of intracellular Ca^{2+}

Increases in intracellular calcium concentration ($[Ca^{2+}]_i$) were determined using fura-2/AM [3]. HEK293 cells stably expressing kB1R or kB2R or primary BPAEC were grown on polylysine-coated glass coverslips to 80% confluence, and then loaded with 2 μM fura-2/AM for 60 min at 37 °C. Cells were washed and then stimulated with various concentrations of kB1R or kB2R agonists as indicated and the fluorescence emission at 510 nm was monitored after excitation at 340 and 380 nm using a PTI Deltascan microspectrofluorometer. Area under the curve was integrated using Origin 8.0 software (OriginLab Corporation). EC_{50} was calculated by plotting the dose-response curve based on the area under the curve of the calcium response using GraphPad Prism 5.0 software.

2.6. Phosphoinositide turnover assay

Phosphoinositide (PI) turnover was determined as previously described [36] with slight modification. Cells at about 80% confluence in 12-well plates were labeled for 18–24 h with 1 μCi/ml of myo-[^{3}H]inositol in DMEM with 2% dialyzed FBS. After loading, the cells were preconditioned with 15 mM LiCl for 60 min at 37 °C, then stimulated with agonists for 30 min at 37 °C followed by termination with 0.5 ml of ice-cold 20 mM formic acid. After 30 min on ice, the supernatant was combined with another 0.5 ml of 20 mM formic acid, alkalinized with 0.2 ml of 3% ammonium hydroxide solution and then applied to an AG 1-X8 anion exchange column. The column was washed with 2 ml of 20 mM formic acid, 4 ml of 50 mM ammonium solution, and then 4 ml of 40 mM ammonium formate containing 0.1 M formic acid. After washing, inositol triphosphate (IP3) was eluted using 5 ml of buffer containing 2 M ammonium formate and 0.1 M formic acid. The eluate was mixed with 10 ml of scintillation fluid and the radioactive IP3 was measured in a Beckman liquid scintillation counter.

2.7. Determination of arachidonic acid

Arachidonic acid release was measured according to a protocol previously described with modifications [37]. Briefly, cells at ~80% confluence were cultured for 18–24 h in growth medium containing 0.1% FBS and 1 μCi/ml [^{3}H]arachidonic acid. After loading, cells were washed three times with HAM's/F12 buffer (10.6 g/L HAM's/F12, 6 g/L HEPES, 1.6 g/L NaHCO$_3$ and 0.1% (w/v) fat-free BSA), and then incubated in HAM's/F12 buffer containing receptor agonist for 30 min at 37 °C. [^{3}H]arachidonic acid released into the medium was counted in a Beckman liquid scintillation counter. EC_{50} was determined using GraphPad Prism 5.0 software.

2.8. Competitive binding assay

Monolayers (80% confluent) of HEK cells stably expressing kB1R or kB2R in 24-well plates were rinsed three times with PBS and incubated with 4 nM of [3H]DAKD or 1 nM [3H]BK and various concentrations of K^9-BK or K^{10}-KD for 90 min on ice. The incubation was stopped by rinsing the cells three times with ice-cold PBS which were then lysed in 0.4 ml of 0.2 M NaOH and transferred to a liquid scintillation vial. The bound [3H]DAKD was measured in a Beckman liquid scintillation counter [36]. The data were analyzed using GraphPad Prism 5.0 software with competitive binding program (one site) (GraphPad Software, Inc.).

2.9. Endocytosis assay

kB2R internalization was determined as previously described by Prado et al. [38] with slight modification. Confluent monolayers of HEK cells stably expressing kB2Rs in 24-well plates were rinsed three times with warm PBS and then incubated with PBS alone (control) or PBS containing 1 µM BK or KD or 10 µM K^9-BK or K^{10}-KD for various times at 37 °C. The cells were washed once with acidified DMEM (pH 2.0) for 5 min, and then washed twice with ice cold PBS. After washing, cells were incubated with 1 nM [3H]BK for 90 min on ice, then washed three times with ice-cold PBS. Cells were lysed in 0.4 ml of 0.2 M NaOH and transferred to a scintillation vial and counted in a Beckman liquid scintillation counter. The internalization of kB2R was calculated as: Fractional endocytosis = (Total binding − residual binding)/Total binding. Total binding = [3H]BK bound to cells incubated with PBS alone. Residual binding = [3H]BK bound to cells treated with cold agonists.

2.10. Western blotting

Cells were lysed in RIPA buffer (20 mM Tris-HCl, pH 7.5, 150 mM NaCl, 1 mM EDTA, 1% NP-40, 1% sodium deoxycholate, 1% protease inhibitor cocktail) with sonication for 30 sec on ice. After centrifugation at 14,000 g for 10 min, the supernatant was collected, mixed with an equal volume of 2X concentrated loading buffer and boiled for 5 min. The protein samples were separated on an 8% SDS-polyacrylamide gel and transferred to a PVDF membrane. The blots were blocked with 5% nonfat dry milk in PBS with 0.5% Tween-20 (PBST) for 2 h at room temperature. The membranes were washed with the same buffer and incubated with primary antibodies overnight at 4°C. Anti-rabbit (Pierce) peroxidase-conjugated secondary antibody was added to the membranes at a dilution of 1:3000 and incubation was continued for 1.5 h at room temperature. The bands were visualized by chemiluminescence (Pierce) [3].

2.11. Determination of ERK1/2 phosphorylation

Cells (80–90% confluent) stably expressing kB1R or kB2R in 24-well plates or primary HLMVEC or BPAEC were stimulated with various concentrations of agonists for 5 min, or with same concentration of agonists for different times. After stimulation, cells were lysed in 200 µl RIPA buffer containing 1 mM sodium orthovanadate (Na_3VO_4) for 5 min on ice. The supernatants were collected after centrifuging at 14,000 g for 10 min (4 °C). The phosphorylated ERK1/2 and total ERK1/2 were identified by Western blotting as described above, and quantified by densitometry using software Quantity One (4.4.0, Bio-Rad). Phosphorylated ERK1/2 was normalized to the corresponding total ERK1/2 band. Data are expressed as fold-increase over the value for the non-treated control. EC_{50} was calculated using GraphPad Prism 5.0 (GraphPad Software, Inc.). For the time course, data are expressed as percentage of the maximum response.

2.12. Determination of kinin peptide hydrolysis by HPLC

HEK cells stably expressing kB1R or CPM were cultured in 12-well plates. After reaching confluency, cells were washed and medium was replaced with PBS. The cells were then incubated with 200 μl of 10 μM K^9-BK, K^{10}-KD or BK for 30 min at 37 °C. The buffer was collected, and then acidified with trifluoroacetic acid (6 μl). The kinin peptides and their cleaved products were separated and quantified by HPLC as previously described [27].

2.13 Measurement of nitric oxide (NO) Production

HLMVEC were treated without ("control") or with 5 ng/ml IL-1β and 100 U/ml IFN-γ for 16 h ("cytokine-treated") to induce kB1R and iNOS expression[39, 40]. Cells were pretreated for 30 min with vehicle or indicated concentration of antagonists HOE140 (kB2R antagonist) or DALKD (kB1R antagonist). Cells were then stimulated with K^{10}-KD and NO production was measured for 20 min in real time with a porphyrinic microsensor as described [39, 41]. The current was proportional to the NO released, and a computer-based Gamry VP600 potentiostat was used to monitor NO concentration over time. Each electrode was calibrated with an NO standard. The concentration of NO achieved at the peak of the initial transient peak and at 20 min after addition of agonist (prolonged response) were both used to quantitate the results.

2.14. Statistical analysis

Data are expressed as means ± SE. For two group comparison, Student's *t*-test was used. The ANOVA was used for more than two group assay, which was followed by Tukey's Test to identify the difference between groups (GraphPad Prism 5.0). Values of $p < 0.05$ were considered significant.

3. Results

3.1. K^9-BK and K^{10}-KD stimulate kB1R signaling

The C-terminal Arg of BK or KD was replaced with lysine, to generate K^9-BK or K^{10}-KD. In HEK cells stably expressing kB1Rs, 10 μM DABK or DAKD stimulated a large increase in $[Ca^{2+}]_i$ whereas 10 μM kB2R agonists BK or KD had no effect (Fig. 1A and B), consistent with the known specificity of the kB1R to bind kinins lacking the C-terminal Arg [2]. Surprisingly, 10 μM K^9-BK or K^{10}-KD also stimulated a large increase in $[Ca^{2+}]_i$, similar to that induced by the kB1R agonists (Fig. 1A and B). Dose response curves for K^9-BK and K^{10}-KD showed the EC_{50} of K^9-BK (1.8×10^{-7} M) and K^{10}-KD (4.7×10^{-8} M) were higher than those of typical kB1R agonists DABK (9.0×10^{-9} M) and DAKD (5.4×10^{-9} M), respectively (Table 2). The response induced by K^9-BK and K^{10}-KD was blocked by specific kB1R antagonist des-Arg^{10}-Leu^9-KD (DALKD) (Fig. 1D). Thus, kinins containing C-terminal Lys are effective kB1R agonists whereas the native kinins BK and KD, containing C-terminal Arg, are not.

In HEK cells expressing kB1Rs, 1 μM K^9-BK and K^{10}-KD also stimulated phosphoinositide (PI) turnover comparable to that induced by same concentration of DABK and DAKD (Fig. 2A). In contrast, BK and KD had no effect (Fig. 2A). Moreover, kB1R antagonist DALKD blocked the PI turnover mediated by K^9-BK and K^{10}-KD indicating a kB1R-specific response (Fig. 2B).

Because kB1Rs are also known to stimulate ERK activation, we also tested the effect of Lys-kinin derivatives on this response. Indeed, K^9-BK and K^{10}-KD also dose-dependently induced ERK1/2 phosphorylation, but the response to K^9-BK was very weak (Fig. 3) and the EC_{50} of K^{10}-KD (7.6×10^{-7} M) was much higher than that of kB1R agonists DABK (4.9×10^{-10} M) and DAKD (2.3×10^{-9} M) (Table 2).

A B-type carboxypeptidase specific for basic residues, such as membrane CPM, can cleave C-terminal Arg from BK or KD [4, 30, 31] and could potentially cleave K^9-BK and K^{10}-KD to generate kB1R agonists DABK and DAKD. However, we previously showed that in HEK cells transfected with only the kB1R, addition of BK or KD did not stimulate a kB1R signal and did not generate DABK or KD unless co-transfected with CPM [3, 27]. In addition, CPM cleaves C-terminal Lys much slower than C-terminal Arg [4, 31, 42]. Nevertheless, to rule out the possibility that kB1R signaling in response to K^9-BK and K^{10}-KD was due to generation of kB1R agonist by removal of the C-terminal Lys, we incubated the peptides for 30 min with HEK cells stably expressing either the kB1R or CPM (as positive control) and analyzed the resulting peptides by HPLC analysis. In experiments with HEK cells expressing only the kB1R, there was no detectable hydrolysis of K^9-BK, K^{10}-KD or BK whereas in cells stably transfected with CPM, 10.1% of K^9-BK, 11.2% of K^{10}-KD and 35.7% of BK were cleaved to the corresponding des-Lys or des-Arg kB1R agonist (not shown). Moreover, in competition binding assays carried out at $4°$ C, which would block peptide hydrolysis, both K^9-BK and K^{10}-KD displaced [^{3}H]DAKD binding to kB1Rs although K^9-BK was much less potent than K^{10}-KD with an IC_{50} of 1.3×10^{-4} M compared with 7.8×10^{-7} M for K^{10}-KD (Fig. 4A).

3.2. K^9-BK and K^{10}-KD also stimulate kB2R signaling

In HEK cells stably expressing kB2Rs, 1 μM K^9-BK or K^{10}-KD stimulated increased $[Ca^{2+}]_i$, with a response similar to that stimulated by 1 μM BK or KD, whereas 1 μM DABK or DAKD (kB1R agonists) had no effect (Fig. 5A and B). The response to K^9-BK and K^{10}-KD was dose-dependent and the potency of the two Lys-kinin derivatives was similar (Fig. 5C) with an EC_{50} for K^9-BK of 1.5×10^{-8} M and for K^{10}-KD of 1.0×10^{-8} M (Table 2). The native kB2R agonist kinins with C-terminal Arg were more potent than the corresponding Lys-derivatives (Fig. 5C; Table 2).

In HEK cells expressing kB2Rs, 1 μM K^9-BK and K^{10}-KD also stimulated PI turnover comparable to that induced by same concentration of BK and KD whereas kB1R agonists DAKD and DABK were ineffective (Fig. 6A). kB2R antagonist HOE 140 blocked the PI turnover mediated by K^9-BK and K^{10}-KD indicating a kB2R-specific response (Fig. 6B).

kB2R activation is known to stimulate the release of arachidonic acid (AA) from membrane phospholipids [43]. In CHO cells stably expressing kB2R-YFP, K^9-BK or K^{10}-KD (1 μM) stimulated AA release as did BK and KD but kB1R agonists DABK and DAKD had no effect (Fig. 7A). Stimulation of AA release in these cells was dose-dependent (Fig. 7B) with an EC_{50} of 1.3×10^{-8} M for K^9-BK and 5.5×10^{-9} M for K^{10}-KD (Table 2), higher than those of BK and KD (Fig. 7B; Table 2). kB2R antagonist HOE 140 also blocked the AA release mediated by K^9-BK and K^{10}-KD (Fig. 7C).

Finally, ERK1/2 phosphorylation mediated by K^9-BK and K^{10}-KD was measured. As shown in Fig. 8, both Lys-derivatives induced ERK1/2 phosphorylation in a dose-dependent manner, although both were less potent than the native peptides BK and KD (Fig. 8; Table 2). In contrast to the calcium response, where K^9-BK and K^{10}-KD had similar potency, K^{10}-KD was over 10-fold more potent ($EC_{50} = 2.9 \times 10^{-9}$ M) than K^9-BK (4.2×10^{-8} M) in stimulating ERK1/2 phosphorylation. However, in the competition binding assays, both K^9-BK and K^{10}-KD displaced [^{3}H]BK binding to kB2Rs with comparable IC_{50}s of 1.6×10^{-9} M for K^9-BK and 3.3×10^{-9} M for K^{10}-KD (Fig. 4B).

3.3. Kinetics of ERK1/2 phosphorylation

The time course of ERK1/2 phosphorylation induced by K^{10}-KD in cells stably expressing kB1Rs was essentially the same as the kB1R agonist DAKD, with a rapid phase peaking at 5

min, followed by a prolonged phase lasting at least 60 min (Figs. 9A and 9B). [Because K^9-BK only weakly induced ERK1/2 phosphorylation in cells stably expressing kB1Rs (Fig. 3 and Table 2), the time course was not determined.]

In cells expressing kB2Rs, the kB2R agonist KD produced a prolonged activation of ERK1/2, peaking at 5 min and very slowly decreasing, with 80% of maximal activation still remaining at 40 min (Figs. 9C and D). BK also stimulated ERK1/2 phosphorylation that was prolonged, although not as robust as that stimulated by KD, with 40% of maximal phosphorylation maintained from 40 – 60 min (Figs. 9E and F). In contrast, the ERK1/2 phosphorylation response to K^{10}-KD also reached a peak in 5 min, but more rapidly returned to baseline within 40 min (Figs. 9C and D). K^9-BK also stimulated peak ERK1/2 phosphorylation at 5 min but the response was even shorter, returning almost to baseline by 20 min (Figs. 9E and F).

3.4. Endocytosis of kB2Rs induced by K^9-BK and K^{10}-KD

kB2Rs are rapidly internalized or sequestered after stimulation with agonists [38]. Treatment of HEK cells stably expressing kB2Rs with BK or KD stimulated rapid endocytosis that was close to maximal by 20 min (Fig. 10). Although K^9-BK and K^{10}-KD also stimulated time-dependent internalization of kB2Rs, the extent of endocytosis was much less. This was especially evident with K^{10}-KD, where maximal endocytosis was only ~20% compared with ~55% endocytosis with KD. The fact that the responses to KD and BK were much more prolonged than K^{10}-KD or K^9-BK indicates that endocytosis is not a major mechanism for terminating the ERK phosphorylation response and may, instead, lead to more prolonged intracellular signaling.

3.5. K^9-BK and K^{10}-KD stimulate both kB1R an kB2R-dependent increased $[Ca^{2+}]_i$ and ERK1/2 phosphorylation in bovine pulmonary artery endothelial cells (BPAEC)

Because cell environment and receptor overexpression can have significant effects on receptor activation and signaling, we tested the ability of K^9-BK and K^{10}-KD to stimulate responses in BPAEC, one of the few cell types that constitutively express both receptors [3, 44, 45]. As shown in Fig. 11, both K^9-BK and K^{10}-KD (1 µM) stimulated a large increase in $[Ca^{2+}]_i$ that was partially blocked by either kB2R antagonist HOE140 or kB1R antagonist DALKD and completely blocked by a combination of both antagonists. We also found that both K^9-BK and K^{10}-KD stimulated ERK1/2 phosphorylation in BPAEC that were pretreated with either kB1R antagonist DALKD (indicating a remaining kB2R response) or kB2R antagonist HOE140 (showing a remaining kB1R response) that was inhibited by a combination of both antagonists (Fig. 12). In both cases, the kB2R response was stronger than the kB1R response as reflected by the greater inhibition with HOE140 (Figs. 11 and 12), consistent with the lower EC_{50} of the lysine derivatives on kB2R responses compared with kB1R (Table 2).

3.6. K^{10}-KD stimulate increased ERK1/2 phosphorylation and NO production in human lung microvascular endothelial cells (HLMVEC)

To further investigate the ability of the lysine-kinin derivatives to stimulate natively expressed kinin receptors, we utilized HLMVEC, which constitutively express kB2Rs and can be induced to express kB1Rs by cytokine treatment [39, 45, 46]. Kinins can stimulate both kB1R and kB2R-dependent ERK1/2 phosphorylation and NO production in these cells [39, 40, 46] (Lowry, J.L. and Skidgel, R.A., unpublished).

In cytokine-treated HLMVEC, K^{10}-KD (1 µM) stimulated an increase in ERK1/2 phosphorylation that was maximal at 5 min (Fig. 13). Pretreatment with kB1R antagonist DALKD appeared to decrease the response, but it did not reach a level of significance.

However, addition of DALKD + kB2R antagonist HOE140 resulted in a significant blockade of the increase in ERK phosphorylation (Fig. 13).

We utilized a porphyrinic microsensor to measure the kinetics of NO output in real time [40, 41, 46] in response to K^{10}-KD. In control HLMVEC, (which express kB2Rs but not kB1Rs), K^{10}-KD (1 μM) stimulated an increase in NO production that was transient, reaching a peak at ~2 – 3 min and then returning to baseline (Fig. 14A), similar to the effect of BK on NO output we previously found in these cells [39]. This response was blocked by kB2R antagonist HOE140, but not kB1R antagonist DALKD (Fig. 14A). In cytokine-treated HLMVEC, (to induce kB1R expression), K^{10}-KD stimulated a transient peak of NO as well as a prolonged phase of NO production (Fig. 14B). We previously showed that kB1R stimulation in cytokine-treated HLMVEC produces a prolonged high output of NO that is due to acute iNOS activation [40, 46]. Indeed, kB1R antagonist DALKD primarily blocked the prolonged phase of NO production, with no effect on the initial transient peak, which was effectively blocked by kB2R antagonist HOE140 (Fig. 14B). HOE140 also partially reduced the prolonged phase of NO production stimulated by K^{10}-KD, consistent with our previous finding of kB2R-dependent prolonged NO production in response to BK in cytokine-treated HLMVEC [39]. These data show that K^{10}-KD stimulates both kB1R and kB2R-dependent NO production in HLMVEC.

4. Discussion

Signaling through the kallikrein-kinin system is mediated by kB1Rs and kB2Rs, GPCRs that regulate a variety of physiological and pathological processes such as blood pressure (vasodilation), normal renal function (natriuresis), inflammation and pain [2, 8–11]. There is great interest in developing agonists and antagonists of kB1Rs and kB2Rs as potential drugs for regulating these processes [9–11, 22, 24, 47, 48]. The agents developed so far selectively modulate either kB1Rs or kB2Rs, including kinin peptide analogues or small organic molecules, except for B9430, which antagonizes both the kB1R and kB2R [2, 21, 24, 25]. Here we found that both K^9-BK and K^{10}-KD effectively activate both kB1Rs and kB2Rs as evidenced by stimulation of PI turnover, increased $[Ca^{2+}]_i$, ERK1/2 phosphorylation, arachidonic acid release and NO production. This was true not only in HEK cells transfected with kinin receptors, but also in primary BPAEC that constitutively express both kB1R and kB2R [3, 44, 45] or HLMVEC that constitutively express kB2Rs and in which kB1R expression can be induced with cytokines [39, 45, 46]. These findings indicate common features for binding to kB1Rs and kB2Rs that could be exploited for development of a single compound that can stimulate or inhibit both receptors.

The crystal structures of the kB1R or kB2R complexed with agonists or antagonists have not been determined, but studies on mutant chimeric receptors and homology modeling have indicated the similarities in the structure of their binding pockets for ligands. For example, a chimeric kB2R containing extracellular loop III of the kB1R only had modestly reduced affinity for BK binding but a ~13-fold increase in affinity for kB1R agonist [49]. The two conserved acidic residues located in extracellular loop III of both receptors were involved in the interaction with the basic N-terminal amino acid of their agonists [49]. In contrast, replacing extracellular loop I or II of the kB2R with corresponding kB1R loops did not affect kB2R functions nor binding of kB1R agonists [49]. Replacement of the sixth transmembrane domain of kB2R with that of the kB1R dramatically reduced BK binding but did not alter the binding of kB2R antagonist NPC17731 [50]. Moreover, homology modeling of B1 and kB2Rs revealed many similar interactions in binding of their agonists or antagonists [51, 52]. These findings support the idea that a single agent can be developed to regulate both kB1R and kB2R functions.

It was reported that ionic interactions provide important binding energy for kB1R and kB2R association with their ligands [2]. For example, one non-peptide antagonist of the kB1R has a simplified common pharmacophore, which has hydrophobic group (such as aryl), a hydrogen-bonding acceptor such as SO_2 or CO, a linker group and a basic group including imidazoline, amines [24]. In fact, a single positive charge in the 3rd transmembrane domain of the kB1R (Lys^{118}) is responsible for repelling the C-terminal Arg of kB2R agonists and thus mediates its selectivity for des-Arg-kinin agonists [53]. In the kB2R, this residue is Ser^{111} which allows interaction with peptides containing C-terminal Arg [53]. Based on these results, it is not surprising that Lys^9 kinins bind and activate kB2Rs, but the ability to activate kB1Rs was unexpected. The reason that Arg^9-kinins do not activate kB1Rs but Lys^9-kinins do is not clear, but may be related to the differences in their side chains. Lys has a longer side chain than Arg and has the greatest side-chain flexibility of all amino acids [54] and may be able to adopt a conformation when bound to the kB1R that largely avoids interaction with Lys^{118} in transmembrane domain 3. In addition, except for the ε-amino group, the side chain of Lys is quite hydrophobic and frequently interacts with other hydrophobic side chains via van der Walls interactions [55]. It thus may be able to participate in the binding normally mediated by the hydrophobic C-terminal Phe in the typical des-Arg kinin kB1R agonists.

It is possible that ligands with dual binding specificity would be advantageous in treating some diseases because kB1Rs and kB2Rs have overlapping signaling, resulting in release of similar mediators (e.g., NO, prostaglandins) and both receptors are present and may participate in many pathophysiological processes [12, 14, 17, 19, 20]. For example, early studies with K^9-BK or K^{10}-KD showed that they stimulate a greater hypotensive response than equal doses of BK and KD after i.v. administration to guinea pigs [56]. Although the EC_{50}s of K^9-BK and K^{10}-KD for human kB2R are higher than those of BK and KD, the greater in vivo effect of K^9-BK and K^{10}-KD in guinea pigs might be due, at least partially, to additional activation of kB1R signaling. Alternatively, K^9-BK and K^{10}-KD might have a higher affinity for guinea pig kB2Rs than human receptors or they may be more resistant to degradation. Effectiveness of kB1R and kB2R agonists or antagonists can be species-dependent and the lifetime of BK and KD in vivo is lower than 30 seconds [2, 9, 21, 24].

The EC_{50}s of K^9-BK and K^{10}-KD are almost 100-fold higher than those of specific kB1R or kB2R agonists (Table 2). However, K^9-BK and K^{10}-KD are not just partial agonists because at high enough concentrations, they can stimulate maximal kB1R and kB2R-mediated calcium responses, equivalent to those of the specific kB1R and kB2R agonists.

The time course of ERK1/2 phosphorylation induced by K^{10}-KD activation of the kB1R was the same as that mediated by kB1R agonist DAKD with a rapid phase peaking at 5 min, followed by a prolonged phase lasting at least 60 min. For several other GPCRs, rapid ERK1/2 phosphorylation has been attributed primarily to G protein-dependent activation whereas prolonged ERK1/2 phosphorylation is mediated by β-arrestin-dependent MAP kinase scaffolding and activation in the cytoplasm [57]. Indeed, we recently showed that the late, prolonged phase of ERK1/2 activation in response to kB1R activation required for high output iNOS–derived NO production is dependent on β-arrestin 2 [58]. This is consistent with the results of the present study showing a kB1R-dependent prolonged phase of ERK1/2 activation with either K^{10}-KD or DAKD.

In contrast, the time course of ERK1/2 phosphorylation stimulated by K^{10}-KD and K^9-BK acting on kB2Rs was quite different from that induced by kB2R agonists KD and BK (Fig. 9). Peak ERK1/2 phosphorylation was at 5 min for all agonists, but the responses to the Lys^9-kinins dropped more rapidly, reaching baseline by 20 – 40 min whereas with the native Arg^9-kinins, ERK1/2 phosphorylation was prolonged and still at ~40 – 70% of the

maximum at 60 min. Recent studies have found that biased ligands of GPCRs can selectively activate G-protein or β-arrestin mediated signaling [32]. Thus, it is possible that K^{10}-KD and K^9-BK activate the kB2R to stimulate primarily G protein-dependent ERK1/2 phosphorylation whereas KD and BK stimulate both G protein-dependent and prolonged β-arrestin-dependent ERK activation. Another potential explanation for the different kinetics of kB2R-mediated ERK1/2 phosphorylation is differences in their ability to cause desensitization and endocytosis. Indeed, the more prolonged signaling of kB1Rs compared with kB2Rs has been attributed to their relative resistance to desensitization whereas kB2Rs are generally rapidly desensitized [2, 59]. However, this does not explain the difference in kinetics of ERK1/2 activation by these agonists as KD and BK stimulated much greater kB2R endocytosis compared with K^{10}-KD and K^9-BK. Our findings are consistent with the possibility that prolonged ERK1/2 activation requires receptor endocytosis and that signaling continues in a β-arrestin-dependent fashion in endosomes, as shown for other GPCRs [57]. Indeed, although β-arrestin 2 is necessary for kB2R endocytosis and desensitization of G protein-dependent signaling [60, 61], β-arrestin 2 was recently reported to mediate prolonged kB2R-mediated ERK1/2 activation [61]. Based on these findings, our results are consistent with the possibility that natural agonists KD and BK cause both rapid G protein-dependent and prolonged β-arrestin 2-dependent ERK1/2 activation whereas K^{10}-KD and K^9-BK only stimulate the rapid G-proteins dependent phase.

The C-terminal region of the kB2R contains potential phosphorylation motifs for G protein-coupled receptor kinases (GRKs) [2]. Phosphorylation by GRKs is considered to be essential for receptor recruitment of β-arrestin [62]. Biased agonists exist for angiotensin type 1 and μ-opioid receptors [32, 63] and one potential mechanism for their biased effects is the ability to recruit different GRK subtypes to the receptor [64]. Thus, K^{10}-KD and K^9-BK might stimulate G protein-mediated signaling but not β-arrestin-dependent responses due to its inability to induce β-arrestin 2 binding. This type of biased response could be exploited in development of more specific therapeutic agents to interact with the kB2R.

5. Conclusion

In summary, we have identified K^9-BK and K^{10}-KD as agonists of both kB1Rs and kB2Rs that also may represent biased agonists of kB2Rs. These findings provide not only future research tools to dissect receptor signaling, for example biased agonism of kB2Rs, but also provide useful starting points for developing dual modulators of kB1Rs and kB2Rs. The development of low molecular weight compounds that can activate both kB1Rs and kB2Rs, for example to generate nitric oxide [40, 65], might be useful in the treatment of some cardiovascular diseases. Alternatively, development of specific biased agonists for the kB2R might be useful for targeted therapy, where activation of only a subset of kB2R downstream signaling events is desired.

Acknowledgments

Abbreviations

CP	carboxypeptidase
kB1R	kinin B1 receptor
kB2R	bradykinin B2 receptor

$[\text{Ca}^{2+}]_i$	intracellular calcium concentration
PBS	phosphate buffered saline
DMEM	Dulbecco's Modified Eagle's Medium
GPCR	G protein-coupled receptor
BK	bradykinin
KD	kallidin
DABK	des-Arg^9-bradykinin
DAKD	des-Arg^{10}-kallidin
K^9-BK	Lys^9-bradykinin
K^{10}-KD	Lys^{10}-kallidin
DALKD	des-Arg^{10}-Leu^8-kallidin
HEK	human embryonic kidney
FBS	Fetal bovine serum
CHO	Chinese hamster ovary
PI	Phosphoinositide
IP3	inositol triphosphate
RIPA	radio-immunoprecipitation assay
B9430	D-Arg-[Hyp^3, Igl^5, D-Igl^7, Oic^8]-bradykinin
NO	nitric oxide
eNOS	endothelial nitric oxide synthase
iNOS	inducible nitric oxide synthase

References

1. Campbell DJ. Clin Exp Pharmacol Physiol. 2001; 28:1060–1065. [PubMed: 11903316]

2. Leeb-Lundberg LM, Marceau F, Muller-Esterl W, Pettibone DJ, Zuraw BL. Pharmacol Rev. 2005; 57:27–77. [PubMed: 15734727]

3. Zhang X, Tan F, Zhang Y, Skidgel RA. J Biol Chem. 2008; 283:7994–8004. [PubMed: 18187413]

4. Skidgel RA, Davis RM, Tan F. J Biol Chem. 1989; 264:2236–2241. [PubMed: 2914904]

5. Skidgel RA, Tan FL, Deddish PA, Li XY. Biomed Biochim Acta. 1991; 50:815–820. [PubMed: 1801758]

6. Skidgel RA, Erdos EG. Int Immunopharmacol. 2007; 7:1888–1899. [PubMed: 18039526]

7. Marceau F, Hess JF, Bachvarov DR. Pharmacol Rev. 1998; 50:357–386. [PubMed: 9755287]

8. Emanueli C, Madeddu P. Trends Pharmacol Sci. 2001; 22:478–484. [PubMed: 11543876]

9. Calixto JB, Medeiros R, Fernandes ES, Ferreira J, Cabrini DA, Campos MM. Br J Pharmacol. 2004; 143:803–818. [PubMed: 15520046]

10. McLean PG, Perretti M, Ahluwalia A. Cardiovasc Res. 2000; 48:194–210. [PubMed: 11054467]

11. Riad A, Zhuo JL, Schultheiss HP, Tschope C. Curr Opin Nephrol Hypertens. 2007; 16:22–26. [PubMed: 17143067]

12. Madeddu P, Varoni MV, Palomba D, Emanueli C, Demontis MP, Glorioso N, Dessi-Fulgheri P, Sarzani R, Anania V. Circulation. 1997; 96:3570–3578. [PubMed: 9396457]

13. Emanueli C, Maestri R, Corradi D, Marchione R, Minasi A, Tozzi MG, Salis MB, Straino S, Capogrossi MC, Olivetti G, Madeddu P. Circulation. 1999; 100:2359–2365. [PubMed: 10587341]

14. Duka I, Kintsurashvili E, Gavras I, Johns C, Bresnahan M, Gavras H. Circ Res. 2001; 88:275–281. [PubMed: 11179194]

15. Kakoki M, Takahashi N, Jennette JC, Smithies O. Proc Natl Acad Sci USA. 2004; 101:13302–13305. [PubMed: 15326315]

16. Kakoki M, McGarrah RW, Kim HS, Smithies O. Proc Natl Acad Sci USA. 2007; 104:7576–7581. [PubMed: 17452647]

17. Ferreira J, Campos MM, Araujo R, Bader M, Pesquero JB, Calixto JB. Neuropharmacology. 2002; 43:1188–1197. [PubMed: 12504926]

18. Pesquero JB, Araujo RC, Heppenstall PA, Stucky CL, Silva JA Jr, Walther T, Oliveira SM, Pesquero JL, Paiva AC, Calixto JB, Lewin GR, Bader M. Proc Natl Acad Sci USA. 2000; 97:8140–8145. [PubMed: 10859349]

19. Schulze-Topphoff U, Prat A, Prozorovski T, Siffrin V, Paterka M, Herz J, Bendix I, Ifergan I, Schadock I, Mori MA, Van Horssen J, Schroter F, Smorodchenko A, Han MH, Bader M, Steinman L, Aktas O, Zipp F. Nat Med. 2009; 15:788–793. [PubMed: 19561616]

20. Dos Santos AC, Roffe E, Arantes RM, Juliano L, Pesquero JL, Pesquero JB, Bader M, Teixeira MM, Carvalho-Tavares J. J Neuroinflammation. 2008; 5:49. [PubMed: 18986535]

21. Marceau F, Regoli D. Nat Rev Drug Discov. 2004; 3:845–852. [PubMed: 15459675]

22. Abraham WM, Scuri M, Farmer SG. Eur J Pharmacol. 2006; 533:215–221. [PubMed: 16455073]

23. Amblard M, Daffix I, Berge G, Calmes M, Dodey P, Pruneau D, Paquet JL, Luccarini JM, Belichard P, Martinez J. J Med Chem. 1999; 42:4193–4201. [PubMed: 10514289]

24. Chen JJ, Biswas K. Prog Med Chem. 2008; 46:173–204. [PubMed: 18381126]

25. Burkard M, Zuzack JS, Jones S, Francis M, Whalley ET, Stewart JM, Gera L. Immunopharmacology. 1996; 33:186–190. [PubMed: 8856146]

26. Gobeil F, Pheng LH, Badini I, Nguyen-Le XK, Pizard A, Rizzi A, Blouin D, Regoli D. Br J Pharmacol. 1996; 118:289–294. [PubMed: 8735629]

27. Zhang X, Tan F, Brovkovych V, Zhang Y, Skidgel RA. J Biol Chem. 2011; 286:18547–18561. [PubMed: 21454694]

28. Simpson PB, Woollacott AJ, Hill RG, Seabrook GR. Eur J Pharmacol. 2000; 392:1–9. [PubMed: 10748265]

29. Zubakova R, Gille A, Faussner A, Hilgenfeldt U. Int Immunopharmacol. 2008; 8:276–281. [PubMed: 18182240]

30. Skidgel RA. Trends Pharmacol Sci. 1988; 9:299–304. [PubMed: 3074547]

31. Skidgel RA, Erdös EG. Immunol Rev. 1998; 161:129–141. [PubMed: 9553770]

32. Violin JD, Lefkowitz RJ. Trends Pharmacol Sci. 2007; 28:416–422. [PubMed: 17644195]

33. Luttrell LM, Gesty-Palmer D. Pharmacol Rev. 2010; 62:305–330. [PubMed: 20427692]

34. Tan F, Chan SJ, Steiner DF, Schilling JW, Skidgel RA. J Biol Chem. 1989; 264:13165–13170. [PubMed: 2753907]

35. Chen Z, Deddish PA, Minshall RD, Becker RP, Erdos EG, Tan F. FASEB J. 2006; 20:2261–2270. [PubMed: 17077303]

36. Kalatskaya I, Schussler S, Blaukat A, Muller-Esterl W, Jochum M, Proud D, Faussner A. J Biol Chem. 2004; 279:31268–31276. [PubMed: 15161928]

37. Prado GN, Mierke DF, Pellegrini M, Taylor L, Polgar P. J Biol Chem. 1998; 273:33548–33555. [PubMed: 9837936]

38. Prado GN, Taylor L, Polgar P. J Biol Chem. 1997; 272:14638–14642. [PubMed: 9169425]

39. Sangsree S, Brovkovych V, Minshall RD, Skidgel RA. Am J Physiol Heart Circ Physiol. 2003; 284:H1959–1968. [PubMed: 12623793]

40. Zhang Y, Brovkovych V, Brovkovych S, Tan F, Lee BS, Sharma T, Skidgel RA. J Biol Chem. 2007; 282:32453–32461. [PubMed: 17804409]

41. Brovkovych V, Stolarczyk E, Oman J, Tomboulian P, Malinski T. J Pharm Biomed Anal. 1999; 19:135–143. [PubMed: 10698575]

42. Deiteren K, Surpateanu G, Gilany K, Willemse JL, Hendriks DF, Augustyns K, Laroche Y, Scharpe S, Lambeir AM. Biochim Biophys Acta. 2007; 1774:267–277. [PubMed: 17208058]

43. Hecquet C, Biyashev D, Tan F, Erdos EG. Am J Physiol Heart Circ Physiol. 2006; 290:H948–958. [PubMed: 16183725]

44. Wang Q, Patton WF, Hechtman HB, Shepro D. Cell Signal. 1997; 9:595–602. [PubMed: 9429763]

45. Ignjatovic T, Stanisavljevic S, Brovkovych V, Skidgel RA, Erdös EG. Mol Pharmacol. 2004; 66:1310–1316. [PubMed: 15304551]

46. Brovkovych V, Zhang Y, Brovkovych S, Minshall RD, Skidgel RA. J Cell Mol Med. 2011; 15:258–269. [PubMed: 20015194]

47. Campos MM, Leal PC, Yunes RA, Calixto JB. Trends Pharmacol Sci. 2006; 27:646–651. [PubMed: 17056130]

48. Heitsch H. Expert Opin Investig Drugs. 2003; 12:759–770.

49. Fathy DB, Kyle DJ, Leeb-Lundberg LM. Mol Pharmacol. 2000; 57:171–179. [PubMed: 10617692]

50. Leeb T, Mathis SA, Leeb-Lundberg LM. J Biol Chem. 1997; 272:311–317. [PubMed: 8995263]

51. Gieldon A, Lopez JJ, Glaubitz C, Schwalbe H. ChemBioChem. 2008; 9:2487–2497. [PubMed: 18803210]

52. Ha SN, Hey PJ, Ransom RW, Bock MG, Su DS, Murphy KL, Chang R, Chen TB, Pettibone D, Hess JF. Biochemistry. 2006; 45:14355–14361. [PubMed: 17128974]

53. Fathy DB, Mathis SA, Leeb T, Leeb-Lundberg LM. J Biol Chem. 1998; 273:12210–12218. [PubMed: 9575169]

54. Najmanovich R, Kuttner J, Sobolev V, Edelman M. Proteins. 2000; 39:261–268. [PubMed: 10737948]

55. Dyson HJ, Wright PE, Scheraga HA. Proc Natl Acad Sci USA. 2006; 103:13057–13061. [PubMed: 16916929]

56. Erdos EG, Cano G, Yang HY. Biochem Pharmacol. 1967; 16:1035–1041. [PubMed: 6040386]

57. DeWire SM, Ahn S, Lefkowitz RJ, Shenoy SK. Annu Rev Physiol. 2007; 69:483–510. [PubMed: 17305471]

58. Kuhr FK, Zhang Y, Brovkovych V, Skidgel RA. FASEB J. 2010; 24:2475–2483. [PubMed: 20228252]

59. Pizard A, Blaukat A, Muller-Esterl W, Alhenc-Gelas F, Rajerison RM. J Biol Chem. 1999; 274:12738–12747. [PubMed: 10212257]

60. Simaan M, Bedard-Goulet S, Fessart D, Gratton JP, Laporte SA. Cell Signal. 2005; 17:1074–1083. [PubMed: 15993749]

61. Zimmerman B, Simaan M, Akoume MY, Houri N, Chevallier S, Seguela P, Laporte SA. Cell Signal. 2011; 23:648–659. [PubMed: 21145390]

62. Lefkowitz RJ, Shenoy SK. Science. 2005; 308:512–517. [PubMed: 15845844]

63. Koch T, Hollt V. Pharmacol Ther. 2008; 117:199–206. [PubMed: 18076994]

64. Zidar DA, Violin JD, Whalen EJ, Lefkowitz RJ. Proc Natl Acad Sci USA. 2009; 106:9649–9654. [PubMed: 19497875]

65. Kuhr F, Lowry J, Zhang Y, Brovkovych V, Skidgel RA. Neuropeptides. 2010; 44:145–154. [PubMed: 20045558]

Highlights

- Kinin B1 and B2 receptors are important in normal and pathological conditions.

- We tested kinin derivatives containing C-terminal Lys instead of the native Arg.

- Lys^9-bradykinin and Lys^{10}-kallidin effectively activated both B1 and B2 receptors.

- The Lys-kinin derivatives showed biased agonism for B2 receptor activation of ERK1/2.

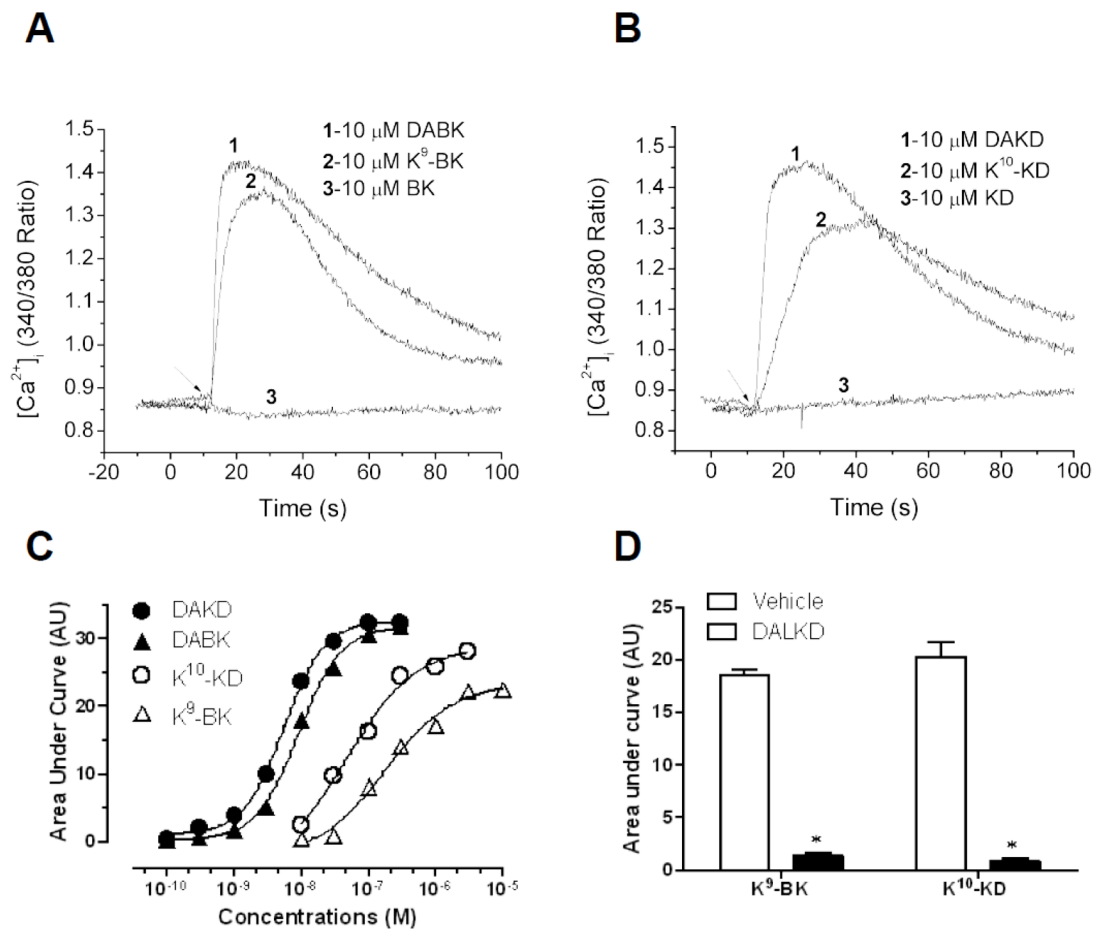- Dual activators of B1 and B2 receptors might be therapeutically useful.

Fig. 1.
K^9-BK and K^{10}-KD stimulate a kB1R-dependent increase in $[Ca^{2+}]_i$. Cells stably expressing the kB1R were stimulated with kinin peptides and the increase in $[Ca^{2+}]_i$ was measured as described in Methods. **A**. Typical tracing showing the increase in $[Ca^{2+}]_i$ mediated by DABK and K^9-BK. kB2R agonist BK had no effect. **B**. Typical tracing showing the increase in $[Ca^{2+}]_i$ stimulated by DAKD and K^9-KD. kB2R agonist KD had no effect. Results shown in **A** and **B** are representative of at least three experiments. **C**. Dose response curves for the kB1R-dependent increase in $[Ca^{2+}]_i$ stimulated by K^9-BK, K^{10}-KD, DABK or DAKD in HEK cells stably expressing kB1Rs. The data are representative of three experiments. **D**. Effect of kB1R antagonist des-Arg^{10}-Leu^9-KD (DALKD) on the increase in $[Ca^{2+}]_i$ induced by K^9-BK or K^{10}-KD. HEK cells stably expressing kB1Rs were pretreated with or without 10 μM DALKD for 60–90 sec. The increased $[Ca^{2+}]_i$ mediated by K^9-BK (1 μM) or K^{10}-KD (1 μM) was recorded and area under the calcium response curve was quantified. The data are expressed as mean ± SE (n=3). *$p < 0.05$, vs vehicle (Student's t test).
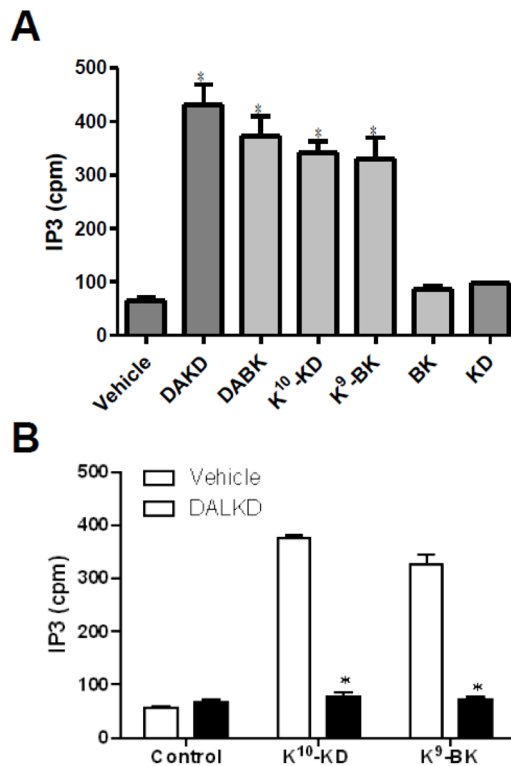
Fig. 2.
K^9-BK and K^{10}-KD induce kB1R-dependent phosphoinositide turnover. **A**. HEK cells stably expressing kB1Rs were treated with 1 μM DABK, DAKD, K^9-BK, K^{10}-KD, BK or KD for 30 min and inositol triphosphate was measured as described in Methods. The data are expressed as mean ± SE (n=4). *p < 0.05, vs vehicle (ANOVA followed by Tukey's test). **B**. HEK cells stably expressing kB1Rs were preincubated with vehicle or kB1R antagonist DALKD (10 μM) for 10 min and cells were then incubated for 30 min with 1 μM K^9-BK or K^{10}-KD and IP3 was measured as in **A**. The data are expressed as mean ± SE (n=4). *p < 0.05, vs vehicle (Student's *t* test).
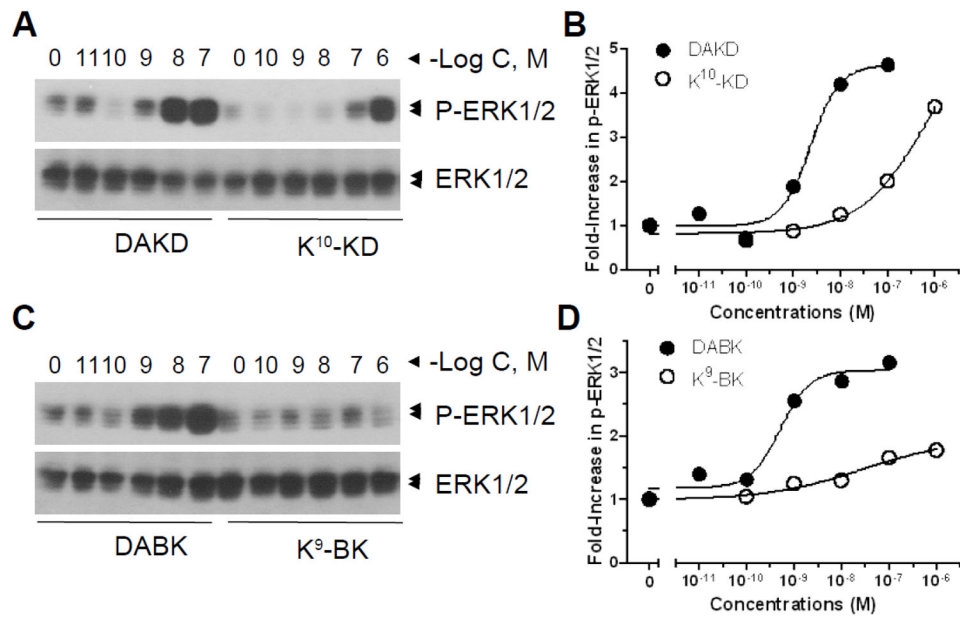
Fig. 3.
K^9-BK and K^{10}-KD dose-dependently induce ERK1/2 phosphorylation through kB1Rs. HEK cells stably expressed kB1Rs were incubated with various concentrations of DABK, DAKD, K^9-BK, or K^{10}-KD for 5 min. Phosphorylated ERK1/2 and total ERK1/2 were detected by Western blotting (**A** and **C**) and quantified by densitometry according to the description in methods. The data are representative of three experiments.
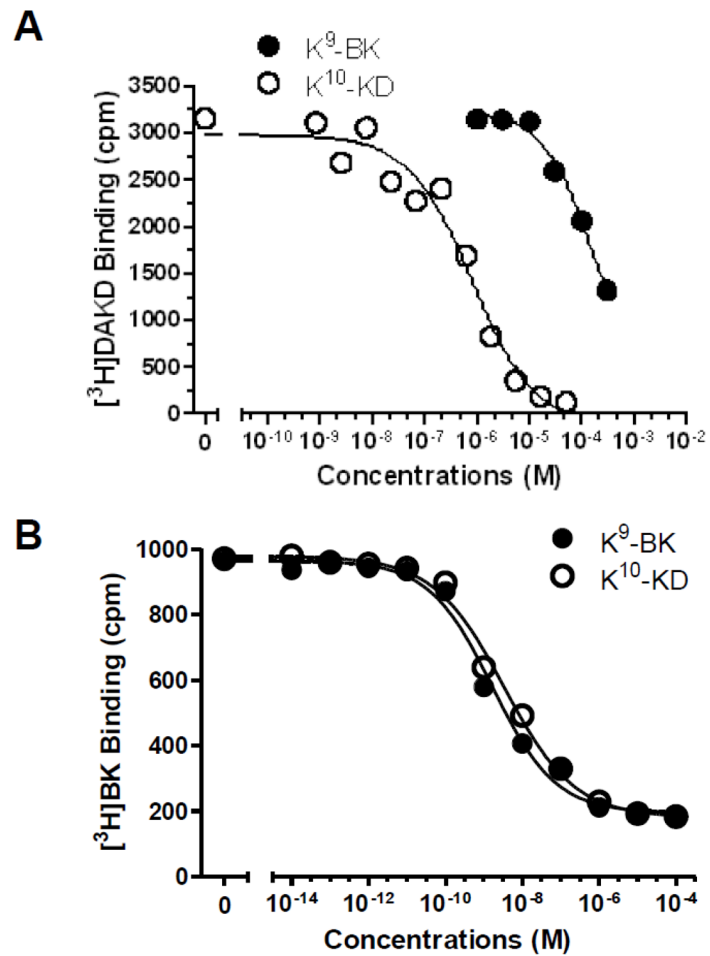
Fig. 4.
K^9-BK and K^{10}-KD compete with specific agonists for binding to the kB1R or kB2R. HEK cells stably expressing kB1Rs (**A**) or kB2Rs (**B**) were incubated with 4 nM [^{3}H]-DAKD (**A**) or 1 nM [^{3}H]-BK (**B**) and various concentrations of K^9-BK or K^{10}-KD for 90 min on ice. After washing, the residual binding of [^{3}H]-DAKD or [^{3}H]-BK were determined by liquid scintillation counting. The data are representative of three experiments.
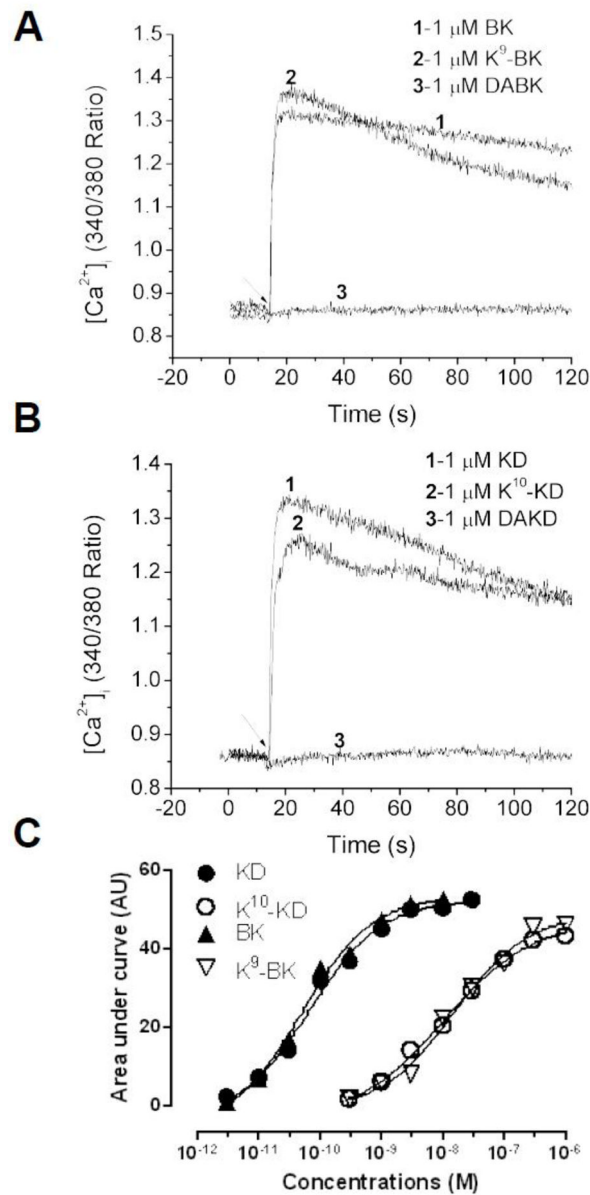
Fig. 5.
K^9-BK and K^{10}-KD stimulate a kB2R-dependent increase in $[Ca^{2+}]_i$. HEK cells stably expressing kB2Rs were stimulated with kinin-related peptides and the increase in $[Ca^{2+}]_i$ was recorded as described in Methods. Typical tracing showing the increase in $[Ca^{2+}]_i$ mediated by BK and K^9-BK. kB1R agonist DABK had no effect. **B**. Typical tracing showing the increase in $[Ca^{2+}]_i$ stimulated by KD and K^9-KD. kB1R agonist DAKD had no effect. Results shown in **A** and **B** are representative of at least three experiments. **C**. Dose response curves for the kB2R-dependent increase in $[Ca^{2+}]_i$ stimulated by K^9-BK, K^{10}-KD, BK or KD in HEK cells stably expressing kB2Rs. The data are representative of three experiments.
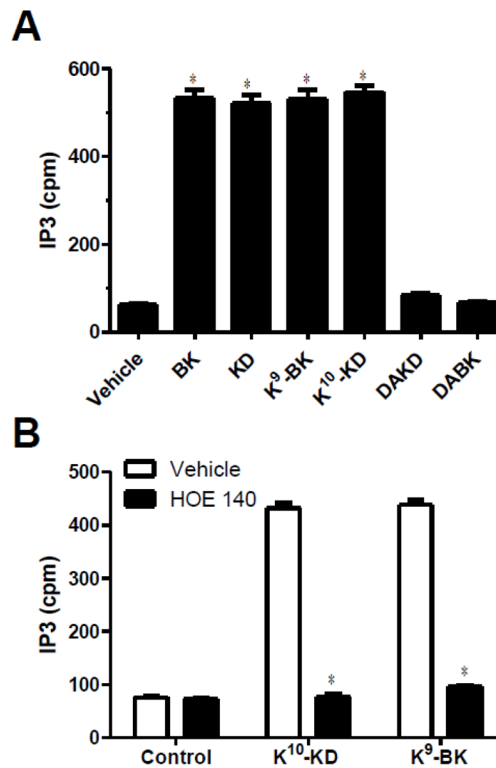
Fig. 6.
K^9-BK and K^{10}-KD induce kB2R-dependent phosphoinositide turnover. **A**. HEK cells stably expressing kB2Rs were treated with 1 μM BK, KD, K^9-BK, K^{10}-KD, DABK or DAKD for 30 min and inositol triphosphate was measured as described in Methods. The data are expressed as mean ± SE (n=4). *p < 0.05, vs vehicle (ANOVA followed by Tukey's test). **B**. HEK cells stably expressing kB2Rs were preincubated with vehicle or kB2R antagonist HOE140 (1 μM) for 10 min and cells were then incubated for 30 min with 1 μM K^9-BK or K^{10}-KD and IP3 was measured as in **A**. The data are expressed as mean ± SE (n=4). *p < 0.05, vs vehicle (Student's *t* test).
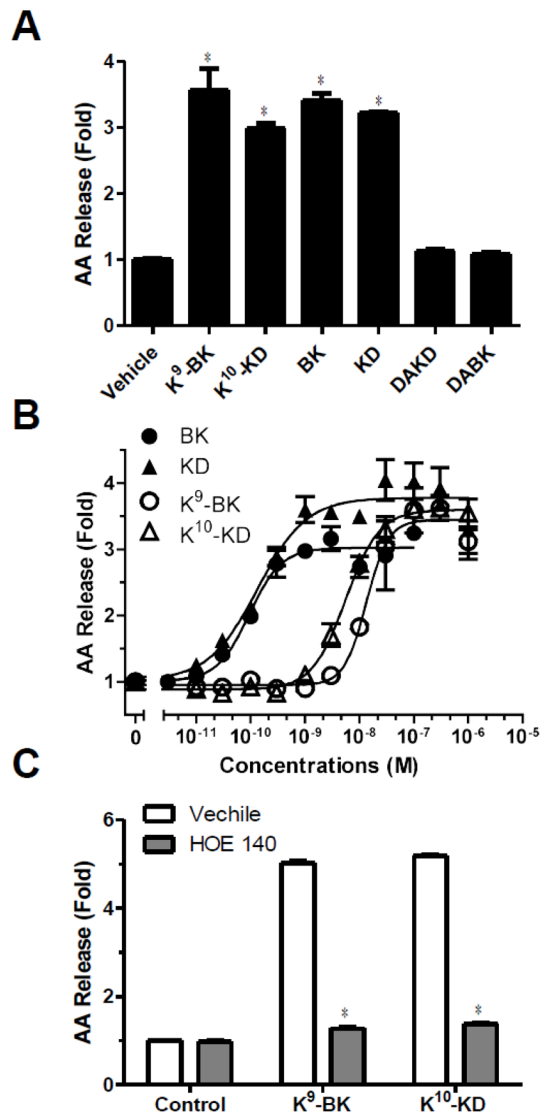
Fig. 7.
K^9-BK and K^{10}-KD stimulate archidonic acid (AA) release by activating kB2Rs. **A**. CHO cells stably expressing kB2R-YFP were incubated with 1 μM K^9-BK, K^{10}-KD, BK, KD, DABK or DAKD for 30 min and AA release was measured as described in Methods. The data are expressed as mean ± SE (n=3). *p < 0.05, vs Vehicle (ANOVA followed by Tukey's test). **B**. CHO cells stably expressing kB2R-YFP were incubated with various concentrations of BK, KD, K^9-BK or K^{10}-KD for 30 min and the AA release was measured. The data are expressed as mean ± SE (n=3). **C**. CHO cells stably kB2R-YFP were incubated with or without 10 μM HOE 140 for 10 min, then the cells were incubated with 1 μM K^9-BK or K^{10}-KD for 30 min and the AA release was measured. The data are expressed as mean ± SE (n=3). *p < 0.05, vs vehicle (Student's *t* test).
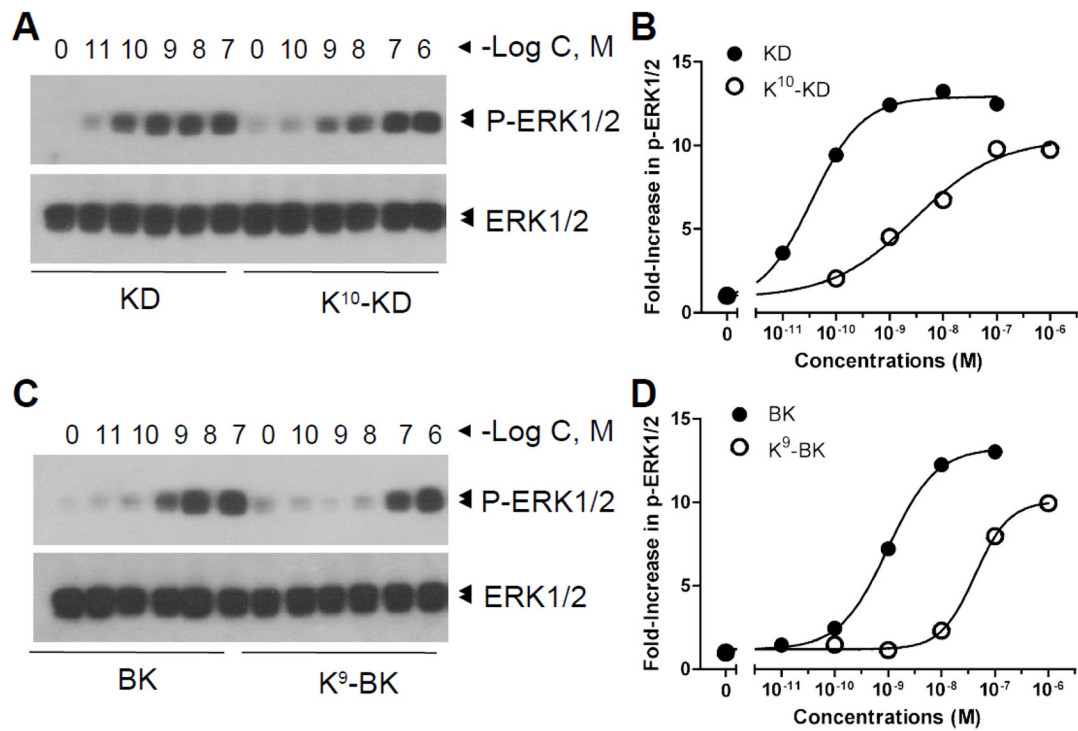
Fig. 8.
K^9-BK and K^{10}-KD dose-dependently induce ERK1/2 phosphorylation through kB2Rs. HEK cells stably expressing kB2R were incubated with various concentrations of KD, K^{10}-KD (**A** and **B**), BK or K^9-BK (**C** and **D**) for 5 min. Phosphorylated ERK1/2 and total ERK1/2 were detected by Western blotting (**A** and **C**) and quantified by densitometry (**B** and **D**). The data are representative of three experiments.
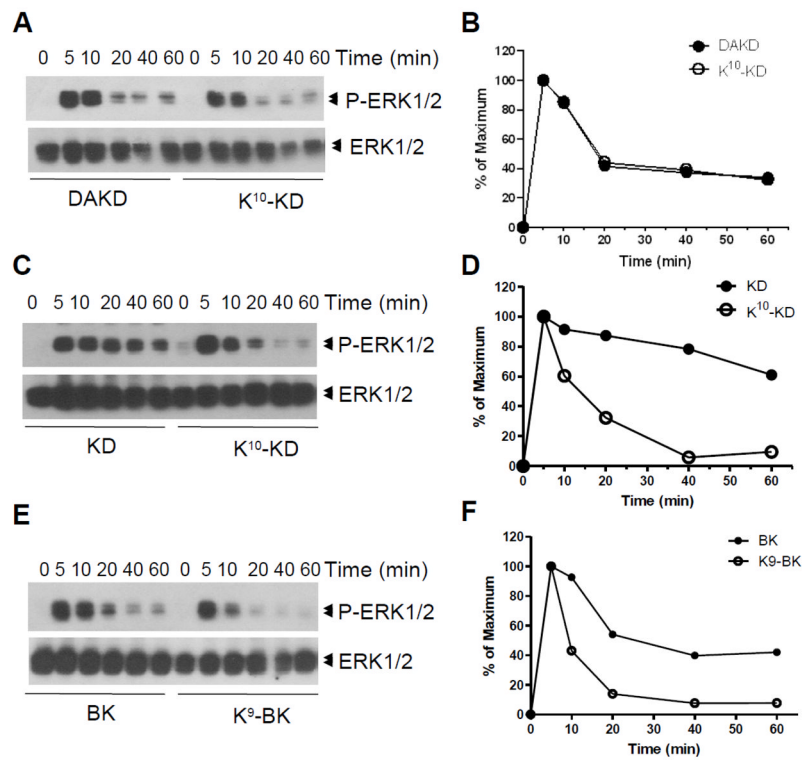
Fig. 9.
The kinetics of ERK1/2 phosphorylation induced by K^{10}-KD or K^9-BK activation of kB1Rs or kB2Rs. HEK cells stably expressing kB1Rs (**A** and **B**) or kB2Rs (**C–F**) were incubated with 1 μM DAKD (**A**), 1 μM KD or BK (**C** and **E**), 10 μM K^{10}-KD (**A** and **C**) or 10 μM K^9-BK (**E**) for various times. Phosphorylated ERK1/2 and total ERK1/2 were detected by Western blotting (**A**, **C** and **E**) and quantified by densitometry (**B**, **D** and **F**). The data are representative of three experiments.
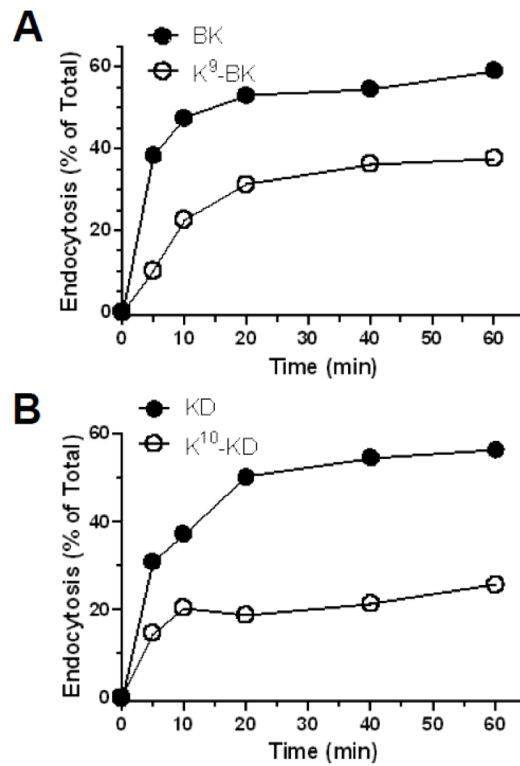
Fig. 10.
Endocytosis of kB2Rs induced by K^9-BK, K^{10}-KD, BK and KD. HEK cells stably expressing kB2Rs were incubated with 10 µM K^9-BK (**A**) or K^{10}-KD (**B**), or 1 µM BK (**A**) or KD (**B**) for various time. After treatment, the fraction of internalized kB2Rs was determined as described in Methods. The data are representative of three experiments.
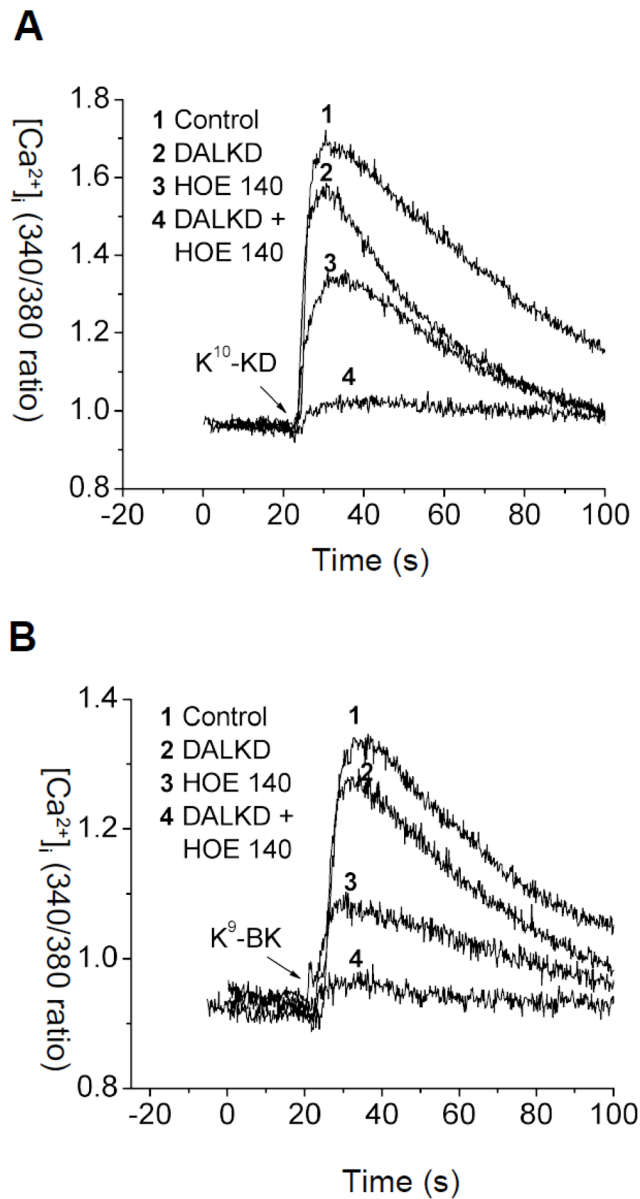
Fig. 11.
K^9-BK and K^{10}-KD stimulate a kB2R- and kB1R-dependent increase in $[Ca^{2+}]_i$ in primary bovine endothelial cells. BPAEC were pre-treated with vehicle (Control) or 10 µM DALKD (kB1R antagonist), 10 µM HOE 140 (kB2R antagonist) or both for 10 min. The increase in $[Ca^{2+}]_i$ was measured after addition of 1 µM K^{10}-KD (**A**) or K^9-BK (**B**). The results are representative of three experiments.
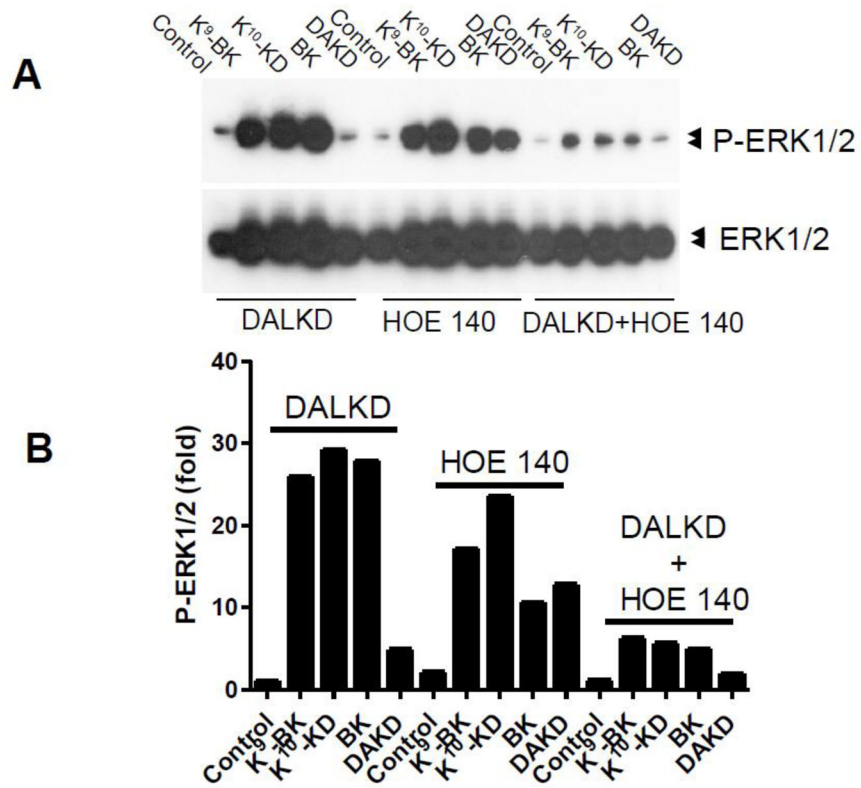
Fig. 12.
K^9-BK and K^{10}-KD stimulate a kB2R- and kB1R-dependent increase in ERK1/2 phosphorylation in primary bovine endothelial cells. BPAEC were pre-treated with 10 μM DALKD (kB1R antagonist), 10 μM HOE 140 (kB2R antagonist) or both for 10 min followed by addition of 1 μM K^{10}-KD, K^9-BK, DAKD (kB1R agonist) or BK (kB2R agonist) for 5 min. The phosphorylated and total ERK1/2 were determined by Western blotting (**A**) and the blot shown was quantified by densitometry (**B**). The data are representative of three independent experiments.
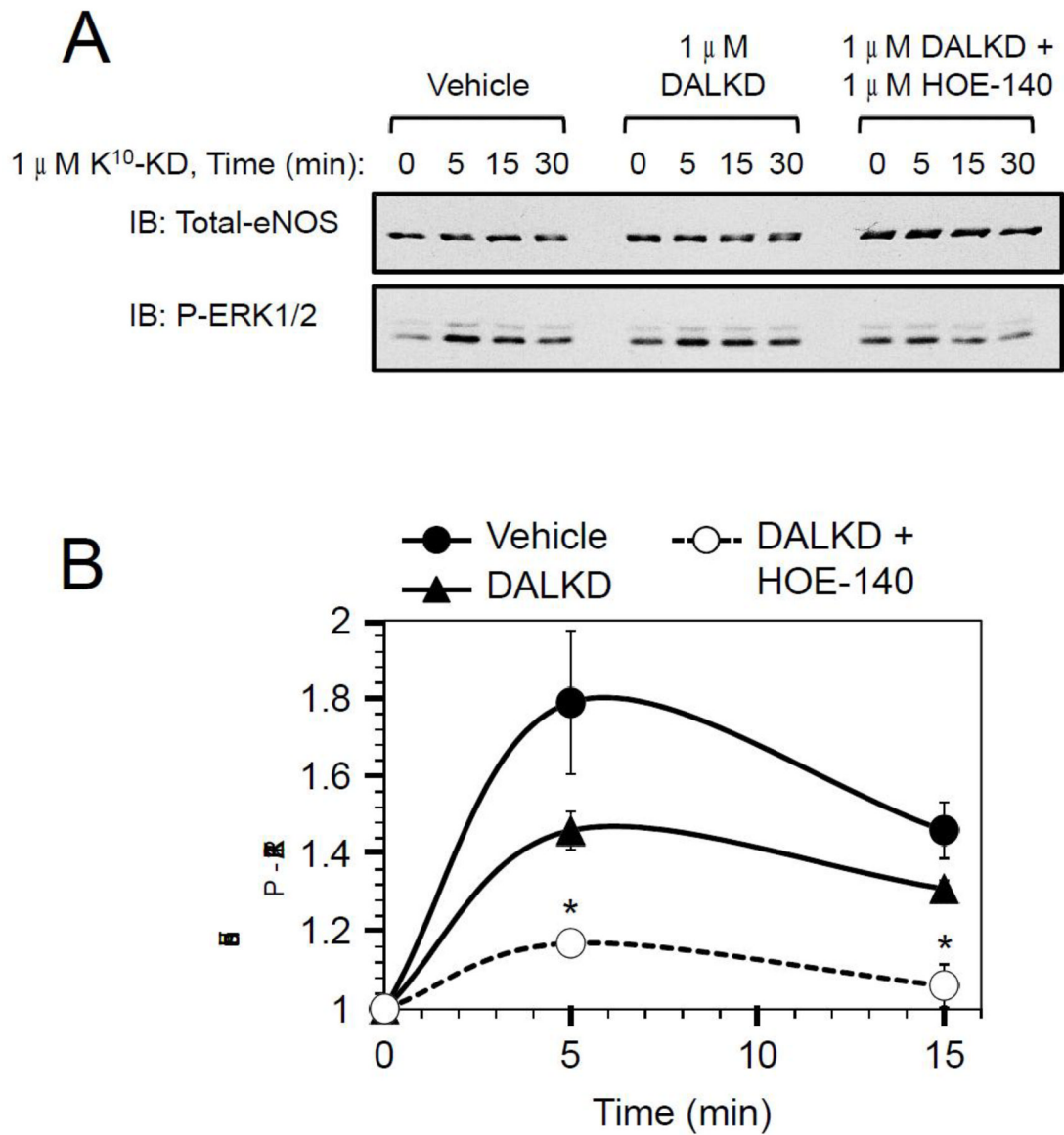
Fig. 13.
Stimulation of ERK1/2 phosphorylation by K^{10}-KD in primary human endothelial cells. Cytokine-treated HLMVEC were pre-treated for 20 min with 20 μM MGTA (CPM inhibitor) and either vehicle, 1 μM DALKD or 1 μM DALKD + 1 μM HOE 140. Cells were then stimulated with 1 μM K^{10}-KD for the indicated times. (**A**) Phosphorylated ERK1/2 and total eNOS (as a loading control) were determined by Western blotting. (**B**) Densitometry analysis of phospho-ERK1/2 was determined in 3 independent experiments and quantified by densitometry (**B**). The data are expressed as mean ± SE (n=3). *p < 0.03 vs vehicle (Student's *t* test).
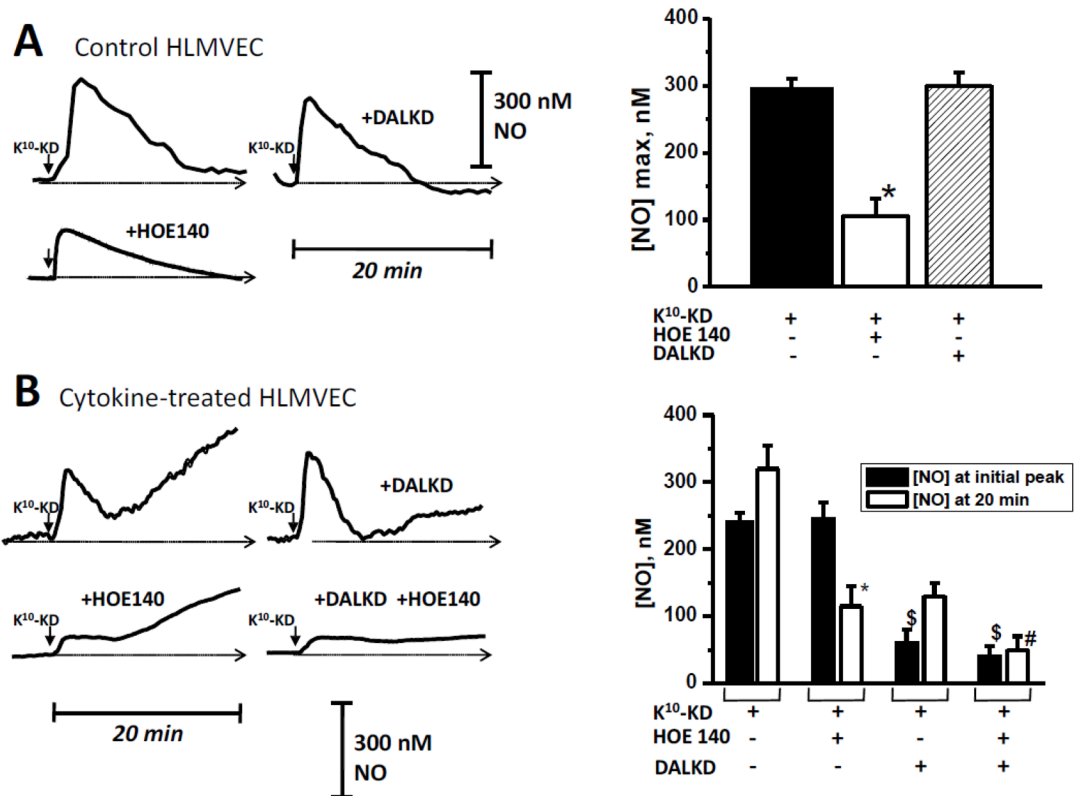
Fig. 14.
K^{10}-KD stimulates a kB2R- and kB1R-dependent increase in NO production in primary human endothelial cells. (**A**) HLMVEC were pre-incubated for 30 min with 1 μM HOE140 or 1 μM DALKD. K^{10}-KD (100 nM) was added and NO was measured in real time for 10 min with a porphyrinic microsensor. *Left:* Example of real time NO tracing. Scale bar shows electrode response to 300 nM NO standard. *Right:* Results were quantitated and mean values ± SE (n = 3) are shown. (**B**) HLMVEC pretreated with 5 ng/ml IL-1β and 100 U/ml IFN-γ for 16 h ("Cytokine-treated") were pre-incubated for 30 min with 10 μM HOE140 or 10 μM DALKD. K^{10}-KD (1 μM) was added and NO was measured in real time for 20 min with a porphyrinic microsensor. *Left:* Example of real time NO tracing. Scale bar shows electrode response to 300 nM NO standard. *Right:* Results were quantitated both by measuring the maximum NO concentration of the initial peak and by the NO concentration achieved at 20 min. Shown are mean values ± SE (n = 3). * = $p < 0.05$ vs K^{10}-KD alone; $ = $p < 0.05$ vs K^{10}-KD or K^{10}-KD + DALKD; # = $p < 0.05$ vs K^{10}-KD or K^{10}-KD + HOE140.

Table 1

Sequences of peptides used.

Peptide	Amino Acid Sequence
Bradykinin (BK)	Arg-Pro-Pro-Gly-Phe-Ser-Pro-Phe-Arg
Lys^9-bradykinin (K^9-BK)	Arg-Pro-Pro-Gly-Phe-Ser-Pro-Phe-Lys
Des-Arg^9-bradykinin (DABK)	Arg-Pro-Pro-Gly-Phe-Ser-Pro-Phe
Kallidin (KD)	Lys-Arg-Pro-Pro-Gly-Phe-Ser-Pro-Phe-Arg
Lys^{10}-kallidin (K^{10}-KD)	Lys-Arg-Pro-Pro-Gly-Phe-Ser-Pro-Phe-Lys
Des-Arg^{10}-kallidin (DAKD)	Lys-Arg-Pro-Pro-Gly-Phe-Ser-Pro-Phe
Des-Arg^{10}-Leu^9-kallidin (DALKD)	Lys-Arg-Pro-Pro-Gly-Phe-Ser-Pro-Leu
HOE 140 [*]	D-Arg-Arg-Pro-Hyp-Gly-Thi-Ser-Tic-Oic-Arg

[*] Hyp, *trans*-4-hydroxy-Pro; Thi, β-(2-thienyl)-Ala; Tic, [D]-1,2,3,4-tetrahydroisoquinolin-3-yl-carbonyl; Oic, (3as,7as)-octahydroindol-2-yl-carbonyl.

Table 2

EC$_{50}$ of K^9-BK and K^{10}-KD in cells stably expressing B1Rs or B2Rs.

	B1R (EC$_{50}$, M)		B2R (EC$_{50}$, M)		
	[Ca^{2+}]$_i$	p-ERK1/2	[Ca^{2+}]$_i$	AA	p-ERK1/2
DAKD	5.4×10^{-9}	2.3×10^{-9}	n.d.	n.d.	n.d.
DABK	9.0×10^{-9}	4.9×10^{-10}	n.d.	n.d.	n.d.
K^{10}-KD	4.7×10^{-8}	7.6×10^{-7}	1.0×10^{-8}	5.5×10^{-9}	2.9×10^{-9}
K^9-BK	1.8×10^{-7}	$>1.0\times10^{-6}$	1.5×10^{-8}	1.3×10^{-8}	4.2×10^{-8}
KD	n.d.	n.d.	6.8×10^{-11}	1.3×10^{-10}	3.5×10^{-11}
BK	n.d.	n.d.	5.0×10^{-11}	9.3×10^{-10}	4.7×10^{-10}

Measurements of increased [Ca^{2+}]$_i$ or phospho (p)-ERK1/2 were in HEK cells and arachidonic acid (AA) release from CHO cells. n.d. = not determined; EC50, half maximal effective concentration.